EFFECT OF CHANNEL THERMAL HYDRAULIC CONDITIONS ON BUNDLE MOTION DUE TO REVERSE FLOW

N.N.Wahba

Ontario Hydro, Reactor Safety and Operational Analysis Department
700 University Avenue, Toronto, Ontario, M5G-1X6

ABSTRACT

If a break should occur in the inlet feeder or inlet header of a CANDU reactor, the rapid depressurization will cause the channel flow(s) to reverse. Depending on the gap between the upstream bundle and shield plug, the string of bundles will accelerate in the reverse direction and impact with the upstream shield plug. The effects of the channel thermal hydraulic conditions on the bundle movement due to reverse flow are investigated. These conditions include channel power as well as enthalpy and pressure of inlet and outlet headers.

1. INTRODUCTION

In CANDU reactors, the fuel channels contain "strings" of 12 or 13 bundles, depending on the channel design. During normal operation, the channel flow forces the bundles in a channel towards the downstream end where they rest against either the downstream shield plug or fuel latch. A small gap, typically less than 0.1 m, exists between the end bundle and upstream shield plug. However, the gap increases over the lifetime of the reactor, due to pressure tube creep, and may become as large as 0.3 m. Also, during abnormal situations, and for a short period of time for single-ended refuelling modes, fewer than the full complement of bundles may be present in a channel and the gap can be significantly larger. When a break occurs in the upstream (i.e., inlet) feeder, the rapid depressurization will cause the channel flow to reverse forcing the string of bundles to accelerate and impact with the upstream shield plug. The potential for bundle and channel damage depends on the bundle velocity at impact.

In some postulated loss-of-coolant accidents (LOCAs) in a CANDU reactor, a rapid relocation of the fuel bundles may occur. If the channels are fuelled in a direction opposite to the coolant flow, the irradiation distribution along the channel is such that the least irradiated fuel resides nearest the downstream end. Therefore, in the event of fuel string displacement towards the upstream end of the channel, fuel with lower irradiation (i,e., at the downstream end) moves into a higher neutron flux region while fuel with higher irradiation (i.e., at the upstream end) moves into a lower flux region. The net result is a positive insertion of reactivity.

A series of five reverse flow, bundle acceleration experiments has been conducted at Stern Laboratories Inc., simulating a break in the inlet feeder of a CANDU fuel channel with 37-element bundles for full power and zero power hot conditions [1,2]. The experimental apparatus consisted of a full scale reactor channel with end-fittings and feeders. The break was simulated using a rupture disc and bundle velocities were measured using a system of magnets and coils. The tests covered the range from a full complement of 13 bundles, with an initial bundle-to-shield plug gap of 0.202 m, to the case of 6 bundles missing with a gap of 3.172 m.

Similar behaviour was observed in all tests. The bundles were observed to accelerate rapidly at first and then level off to a constant or asymptotic value after a few hundred milliseconds, unless the transient is terminated by impact with the shield plug. The experiments show that the bundle string essentially moves as a unit. However, in one of the tests, there was evidence of significant bundle separation due to high initial outlet temperature which resulted in a high voiding following rupture. Bundle separation would distribute the momentum transfer of the bundles to the shield plug over time which could lessen the damage to fuel bundles and fuel channel.

A model, SOPHT-RFI [2,3] has been developed to predict the bundle motion due to the channel flow reversal. The model is a modification of the fully transient, two-phase thermal hydraulic code, SOPHT [4], to incorporate the interaction and feedback between bundle motion and channel thermal hydraulics. The model has been extensively modified to account for various forces acting on the bundle due to reverse flow [3]. These forces result from the pressure gradient, drag and friction between the bundles and the pressure tube. The calculational control volumes of nodes are adjusted to account for the location and velocity of the bundle.

The analytical model has been validated against the experiments. The agreement between measured and predicted velocities is excellent (less than 5.6 percent difference), for all tests with the exception of test 4 where the model over-predicts the impact velocity by about 28 percent. The over-prediction, in test 4, may be attributed to the analytical assumption that the bundles are considered as one solid string whereas the measurements indicated that a significant separation occurred among the first four bundles. Separation between bundles may result in a lower pressure in the gap created between separated bundles, for a short period of time, compared to the no separation case. This may result in a lower acceleration and velocity of the first bundles in comparison with the no separation case.

The details of the code modifications as well as a comparison between measured and predicted values are given in Reference 3. It was also demonstrated that the model may be successfully used to simulate the thermal hydraulic transient and bundle movement in the fuel channel following a large break LOCA or, in the case of a guillotine break at the inlet feeder [3].

The reverse flow impact velocities, in the case of a guillotine break at the inlet feeder, were determined for Bruce NGS A under various reactor operating states using the validated model SOPHT-RFI [5]. The information is needed to support operation with less than a full complement of bundles in the channel and is also required to support channel defuelling. The impact velocities may be used to evaluate channel component integrity analysis. For the case of Full Power, operating with six missing bundles (i.e. seven bundles are present) yields the largest kinetic energies of 14.17 and 13.42 kJ, at impact, as well as the largest impact velocities of 13.07 and 12.72 m/s for inner and outer zones, respectively.

The main parameters affecting the bundle movement due to reverse flow are discussed in Section 2. The analytical model accounting for various forces acting on the bundle due to reverse flow is summarized in Section 3. The analytical model is used to simulate the thermal hydraulic transient in a single channel and predict the bundle movement to assess the effects of the channel thermal hydraulic conditions on the bundle impact velocity. The simulation and analytical results are illustrated in Sections 4 and 5, respectively. Summary and conclusions are presented in Section 6.

2. MAIN PARAMETERS AFFECTING BUNDLE MOVEMENT

The model may be used to simulate the thermal hydraulic transient and bundle movement in a single channel in the case of a guillotine break at the inlet feeder. The bundle motion depends, in general, on the reactor conditions, channel geometry as well as the size and location of the break. The main parameters that affect the bundle movement due to the flow reverse are:

(1) The initial channel thermal hydraulic conditions including channel power and flow, pressure distribution, and coolant temperature profile;
(2) The gap between the first bundle and the shield plug (nominal gap added to the length of the missing bundles);
(3) The bundle loss factor;
(4) The characteristics of the outlet feeder;
(5) The characteristics of the inlet feeder;
(6) The characteristics of the end-fittings;
(7) The size of the break (diameter of the inlet feeder);

(8) The location of the break (distance between the break and the inlet end-fitting);
(9) The duration of the guillotine break to be developed;
(10) The mass of the fuel bundle; and
(11) The friction between the bundles and the pressure tube.

Channel elevation, length and loss coefficient of inlet feeder, and the developing time of the break have an insignificant effect on the bundle motion. Channels with minimum outlet feeder resistance, largest inlet feeder diameter and break located just upstream of the inlet end-fitting give the largest impact velocity. Reducing the end-fitting resistance or increasing the bundle loss coefficient yields larger impact velocity [6].

The bundle velocities depend on the reactor operating conditions such as channel power as well as coolant pressure and temperature. The model was used in predicting the impact velocity and kinetic energy following a guillotine break at the inlet feeder for Bruce NGS A under various reactor operating states [5]. Four different operating states were considered. These states include full power, zero power, shutdown hot and shutdown cold. The initial temperature profile across the channel is flat for all cases, with the exception of the full power case. The outlet header pressure is relatively smaller (about 4 MPa) for shutdown cases than that (about 9 MPa) for full and zero power cases. The inlet header temperature is about 50°C for the shutdown cold case while it is about 260°C for the other cases.

Channels M04 and C12, with a minimum outlet feeder resistance and having the largest inlet feeder cross-sectional area of 0.0031114 m^2, were selected to represent the inner and outer zones, respectively. They are expected to have maximum impact velocity. The gap between the end bundle and the shield plug is assumed to be 0.3 m when all of the thirteen bundles are present. The mass of each bundle is 23.7 kg.

The impact velocity as well as kinetic energy for various numbers of missing bundles are calculated for both inner and outer zones. The maximum kinetic energies, at impact, are 5.45, 5.49, 10.45, 11.83, 14.17 and 13.42 kJ (corresponding to impact velocities of 7.58, 6.49, 9.39, 10.53, 13.07 and 12.72 m/s) for the cases of Shutdown Hot (inner zone), Shutdown Cold (inner zone), Zero Power Hot (inner zone), Zero Power Hot (outer zone), Full Power (inner zone) and Full Power (outer zone), respectively. These results indicate that the value of the impact velocity depends greatly on the channel thermal hydraulic conditions. The effects of the channel thermal hydraulic conditions on the bundle movement due to reverse flow are addressed in Section 5.

3. ANALYTICAL MODEL

The model SOPHT-RFI is an adaption of SOPHT to incorporate the interaction and feedback between bundle motion and channel thermal hydraulics. The equations governing the coolant frictional force and bundle movement are described in detail in Reference [3]. The forces acting on the bundle include: the pressure force F_p, drag force F_d, Coulomb friction force F_c due to friction between bearing pads and pressure tube, damping force, F_D and inertia force F_i. The positive direction of the bundle displacement, velocity and acceleration, coolant flow and forces acting on the bundle, is assumed to coincide with the direction from outlet to inlet feeders.

The pressure force, F_p, arises from the pressure difference at the two ends of the bundle string and acts on the cross-sectional area of the bundle. The drag force, F_d, is caused by the frictional force exerted by the coolant flowing past the bundle and is proportional to the square of the relative velocity between the coolant and the bundle. The drag force acts in the direction of the relative velocity. The friction force due to the contact between the bundle and the pressure tube, F_c, is proportional to the weight of the bundle and acts in the opposite direction of the bundle movement. The damping effect on the bundle motion is attributed to energy dissipation caused by various mechanisms such as structural damping. The equivalent viscous damping force F_D, is proportional to the bundle velocity and acts in the opposite direction of the bundle movement. The force balance of the bundle gives :

$$F_i = F_p + F_d - F_D - F_c$$

The net resultant force represents the inertia force F_i and is used in the calculations of the bundle acceleration. The acceleration of the bundle string is calculated in a separate subroutine based on the predicted drag, dry friction and damping forces as well as pressure drop across the bundle string. The transient velocity as well as motion of the bundle string are also calculated. The bundles in a channel are considered as one solid string. In a time step interval, the forces acting on the bundle string and consequently, the acceleration of the entire string are assumed constant. Then, the bundle velocity at the end of the time step and its displacement during the time step interval are calculated.

The detailed thermal hydraulic model in SOPHT is discussed in Reference [4]. The interaction and feedback between bundle motion and channel thermal hydraulics are incorporated by adjusting the calculational control volumes of nodes and pressure drop along the channel at each time step to account for the location and velocity of the bundle.

The coolant friction factors of the pressure tube and bundles are assumed to be equal. The coolant friction factor and two-phase multiplier are calculated at the coolant thermodynamic conditions using the flow hydraulic diameter based on the overall flow area and total wetted perimeter of both bundle and pressure tube. The coefficient of static friction is about 0.53. A value of 0.25 is used for the dynamic friction coefficient. For the bundle appendages, such as bundle junctions, spacers and bearing pads, the skin friction represents about 11 percent of the total loss factor. The viscous damping force is small and can be neglected [3].

4. SIMULATION

The model is used to simulate the thermal hydraulic transient and bundle movement in a single channel with 37-element bundles in the case of a guillotine break at the inlet feeder. The channel has thirteen bundles. Each bundle has a mass of 23.7 kg, length of 0.495 m and loss coefficient of 0.816. Both feeders are simulated as straight pipes having a constant diameter of 6.3 cm, length of 10 m and loss coefficient of unity. The channel, feeders and end-fittings are finely nodalized. The channel is modelled using two multi-node modules. One module represents the section of the channel occupied by the bundles and the other module represents the section of empty channel. The end-fittings are modelled as an annulus representing the direct flow path between the liner tube and end-fitting wall. The appropriate form loss factors for the end-fittings are used. The gap between the end bundle and the shield plug is assumed to be 0.5 m when all of the thirteen bundles are present. This gap is larger than the maximum gap expected over lifetime pressure tube creep.

The guillotine break at the inlet feeder is assumed to occur just upstream (at 0.5 m) of the inlet end-fitting. This maximizes the pressure drop across the bundle string and consequently, results in the highest bundle velocity. The break is simulated by two break discharge valves and an externally controlled varying resistance link. This resistance link is assigned a large value after the break to cut off flow between the two segments of the feeder at the break location so that the coolant is discharged to atmosphere through the discharge valve. The break is assumed to be completely developed in 30 ms.

For the reference case, the pressures of inlet and outlet headers are 10.4 and 9.2 MPa, respectively. The enthalpy of inlet and outlet headers are 1074 and 1298 kJ/kg, respectively. During the transient, the outlet header pressure and enthalpy are used as fixed constant boundary conditions. In the case of a channel with the full complement of bundles, the channel power is assumed to be 6 MW and cosine axial flux distribution is used. In the case of a channel with less than the full complement of bundles, the channel power is adjusted accordingly.

5. RESULTS AND DISCUSSIONS

The initial channel thermal hydraulic conditions and the characteristics of the break and various channel components are listed in Table 1. These values are used in predicting the bundle impact velocity following a guillotine break at the inlet feeder.

The impact velocity is mainly governed by the bundle/shield plug gap which limits the time over which the bundles can accelerate. The fewer bundles in the channel, the larger the gap, the greater the time available for acceleration and the higher the impact velocity unless the bundles reach the asymptotic limit. The calculations were carried out for different numbers of missing bundles in the channel. The bundle velocities, as functions of time, are shown in Figures 1 and 2. The bundle string accelerates rapidly at first and then levels off (as shown in Figure 2 for 7 or 8 missing bundles), unless the transient is terminated by impact with the shield plug (as shown in Figures 1 and 2, for smaller numbers of missing bundles).

At the onset of the break, the pressure at the break location drops to the saturation pressure corresponding to the inlet header temperature and this results in a large initial pressure force, which accelerates the bundle string. The initial stage is followed by a second stage where the acceleration decreases as the bundles start to move. The second stage starts earlier as the number of missing bundles increases, as shown in Figures 1 and 2. Then, the velocity changes slope and increases again. The reason of this change in the acceleration is due to the transient void and pressure. In some cases, a maximum velocity is reached prior to the impact whereas in others, the transient is terminated by impact with the shield plug. The driving force and consequently the acceleration of the fuel bundles are proportional to the pressure drop across the bundle string and the drag force acting on it. Both forces are proportional to the square of the relative velocity of the coolant flowing through the bundles, i.e., coolant velocity less bundle velocity. As the bundle string accelerates, the relative velocity and therefore the accelerating force, decrease and the bundle string asymptotically approaches a limiting velocity. In cases where only a few bundles are missing from the channel, the bundles may hit the shield plug well before reaching the asymptotic velocity.

The maximum impact velocity is 12.4 m/s and corresponds to the case of five missing bundles (i.e., eight bundles are present). Increasing the number of missing bundles beyond this value results in a lower impact velocity. In this case, the bundle string reaches the limiting velocity before the end of the transient. It can also be concluded that operating with five missing bundles (i.e., eight bundles are present) yields the largest kinetic energy of 14.6 kJ, at impact. The cases of channel operating with the full complement of 13 bundles and with five bundles missing (having maximum kinetic energy at impact) are considered for the study of the sensitivity of the impact velocity to various parameters.

5.1 Channel Power Effect

The level of the channel power determines the initial forward flow, axial temperature distribution and the amount of void along the channel prior to the break. The effect of the channel power on the bundle velocity is illustrated in Figures 3 and 4 for the cases of no and five missing bundles, respectively. At the onset of the break, the pressure at the break location drops to the saturation pressure corresponding to the inlet header temperature and this results in a large initial pressure force, which accelerates the bundle string. Since the inlet header enthalpy is assumed constant for these simulations, the initial stage is the same for all channel power levels. The duration of this stage is short (about 6 ms), which is the time required for the expansion wave, generated by the break, to reach the channel outlet.

In the early portion of the transient, the bundle string velocity becomes larger as the channel power increases, as shown in Figures 3 and 4. During the first stage of the transient, the pressure along the channel drops to the saturation pressure corresponding to the local coolant temperature. This stage is followed by a second stage where the bundle sting acceleration is mainly governed by the pressure gradient along the channel which depends on the initial coolant temperature profile. Since the profile is flat, for the case of zero channel power, no pressure gradient exists along the channel and the acceleration decreases slightly (as shown in Figures 3 and 4), due to the friction between the bundles and the pressure tube. As the channel power increases, the pressure gradient along the channel as well as the bundle string acceleration become greater. Also, increasing the channel power results in a decrease in the initial forward flow and momentum which may result in earlier flow reversal and larger bundle acceleration.

In the case of five missing bundles, the maximum impact velocity is 12.4 m/s and corresponds to channel power of 6 MW. When the channel power is less than 6 MW, the bundle string reaches the limiting velocity before the end of the transient. It can also be concluded that operating with the full complement of bundles yields the largest impact velocity of 6.4 m/s when the channel power is 6 MW.

5.2 Inlet Header Enthalpy Effect

To study the effect of inlet header enthalpy on the bundle motion, calculations were performed for both cases at two values of channel power. The bundle transients are shown in Figures 5 and 6 for zero channel power, and in Figures 7 and 8 for channel power of 6 MW. The channel inlet pressure transient is controlled by the break discharge flow and upstream thermohydraulics. The discharge (choked flow) is strongly dependent on the upstream coolant temperature and void. The minimum pressure to which the inlet feeder drops is directly related to the initial inlet header temperature (or enthalpy), i.e., the lower the initial enthalpy, the lower the pressure and the larger the driving forces acting on the bundle string. Consequently, the initial acceleration increases as the inlet enthalpy decreases, as shown in Figures 5 to 8.

When the channel power is zero, the initial stage of the transient is followed by a second stage where the acceleration is almost zero. During this stage, the axial coolant temperature profile is flat, and no pressure gradient exists along the channel. The duration of the second stage becomes shorter as the inlet header enthalpy decreases, as shown in Figures 5 and 6. At the end of this stage, the pressure gradient along the channel develops and the drag force increases due to flow reversal. Consequently, the acceleration of the bundle string increases.

When the channel power is 6 MW and the inlet header enthalpy is greater than 1000 kJ/kg, the second stage (which is characterized with no bundle acceleration) disappears, as illustrated in Figures 7 and 8. For smaller inlet header enthalpy, the velocity changes slope due to the transient void and pressure. In general, the bundle string reaches the end of the transient earlier having larger impact velocity as the inlet header enthalpy decreases. It should be noted that the effect of inlet header enthalpy on the bundle movement is less pronounced for values less than 800 kJ/kg.

5.3 Outlet Header Enthalpy Effect

The change in outlet header enthalpy has no effect on the initial state of the channel, or on the initial forward flow and momentum. Consequently, its effect on the bundle velocity is insignificant, for the case of no bundle missing and for the early portion of the transient in the case of 5 bundles missing, as illustrated in Figures 9 and 10, respectively. In the latter portion of the transient, the higher temperature coolant from the outlet header flows through the channel and the effect of enthalpy becomes noticeable. In the case of operating with 5 bundles missing, the bundle impact velocity increases from 12.2 to 13.2 m/s as the outlet header enthalpy increases from 1074 to 1500 kJ/kg.

5.4 Channel Pressure Effect

The effect of the channel pressure on the bundle velocity is illustrated in Figures 11 and 12, for the cases of no and five missing bundles, respectively. In these simulations, an inlet header enthalpy of 1074 kJ/kg and a header to header pressure drop of 1.2 MPa are used. At the onset of the break, the pressure at the break location drops to the saturation pressure of 4.4 MPa, corresponding to the inlet header enthalpy. If the outlet header pressure is greater than 4.4 MPa, the bundle string starts to move at the onset of the break, as shown in Figures 11 and 12. Increasing the outlet header pressure yields a larger pressure drop and driving force acting on the bundle string which may result in a higher final bundle velocity.

If the outlet header pressure is less than 4.4 MPa, the bundle string will not start to move until the initial forward flow momentum is overcome by the flow reversal, the pressure gradient along the channel develops and the drag force increases. In this case, decreasing the outlet header pressure yields a larger amount of void and a smaller initial forward flow, and this results in earlier bundle movement, as shown in Figures 11 and 12. Again, increasing the outlet header pressure yields a larger pressure drop and driving force acting on the bundle string. which may result in a higher final bundle velocity. This explains why the bundle string starts to move earlier and has a smaller impact velocity at 2 MPa, as compared with 4 MPa.

5.5 Header to Header Pressure Drop Effect

Two sets of simulations were carried out. In the first set, header to header pressure drop varies by changing the inlet header pressure, whereas the outlet header pressure is maintained constant at 9.2 MPa. Since the guillotine break at the inlet feeder is assumed to occur just upstream of the inlet end-fitting, the inlet header pressure does not play any role during the transient. However, increasing header to header pressure drop results in larger initial forward flow and momentum which may delay the onset of the bundle motion and decrease the bundle string acceleration and consequently, it may result in a lower final bundle velocity. This is evident from the results shown in Figures 13 and 14 for the cases of no and five missing bundles, respectively.

In the second set of simulations, header to header pressure drop varies by changing the outlet header pressure, whereas the inlet header pressure is maintained constant at 10.4 MPa. Again, increasing header to header pressure drop results in larger initial forward flow and momentum which may delay the onset of the bundle motion and decrease the bundle string acceleration and consequently, it may result in a lower final bundle velocity. Also, increasing the outlet header pressure yields a larger pressure drop and driving force acting on the bundle string during the transient. This results in a higher final bundle velocity, as shown in Figures 15 and 16 for the cases of no and five missing bundles, respectively.

6. SUMMARY AND CONCLUSIONS

During normal operation, the channel flow forces the bundle string towards the downstream end where it rests against the fuel latch. A small gap exists between the end bundle and upstream shield plug. When fewer than the full complement of bundles are present in a channel, the gap is larger. In the event that a break occurs in the inlet feeder or inlet header, the rapid depressurization will cause the channel flow to reverse forcing the string of bundles to accelerate and impact with upstream shield plug. In this case, the potential bundle and channel damage depends primarily on the velocity of the bundles at impact. For the case of fuelling against the flow, the bundle relocation due to reverse flow may result in a positive insertion of reactivity.

The reverse flow impact velocities, in the case of a guillotine break at the inlet feeder, are determined using the validated model SOPHT-RFI. The information is needed to support operation with less than a full complement of bundles in the channel and is also required to support channel defuelling. The impact velocities may be used to evaluate channel component integrity analysis.

Removal of one or more of the inlet end bundles would add a gap equal to the length of these bundles to the existing gap and may result in a larger impact velocity. In cases where only a few bundles are missing from the channel, the bundles may hit the shield plug well before reaching the asymptotic velocity. The maximum impact velocity is achieved for a certain number of missing bundles. Increasing the number of missing bundles beyond this value results in a lower impact velocity. In this case, the bundle string reaches the limiting velocity before the end of the transient.

The effects of the channel thermal hydraulic conditions on the bundle movement due to reverse flow are investigated. These results indicate that the value of the impact velocity depends greatly on the channel thermal hydraulic conditions such as channel power as well as enthalpy and pressure of both headers. Increasing the outlet header pressure, reducing the inlet header enthalpy or increasing the outlet header enthalpy yields larger impact velocity.

7. REFERENCES

[1] HADALLER,G.I. and SANDIG,P.F., "Reverse Flow Induced Bundle Impact Velocity Tests", Report SL-020, Stern Laboratories Inc., August 1995.

[2] LOCKE,K.E. and TRAN,F.B.P., "Thermal Hydraulic and Dynamic Modelling of Reverse Flow Bundle Acceleration Experiments", Ontario Hydro, Nuclear Safety Department, Report No. 90331, 1992.

[3] WAHBA,N.N. and AKALIN,O., "Fuel Bundle Movement due to Reverse Flow", 16th Annual Conference, Canadian Nuclear Society, Saskatoon, Saskatchewan, Canada, June 4-7, 1995.

[4] CHANG,Y.F., "Thermal-Hydraulic System Simulation Model for the Reactor, Boiler and Heat Transport System (SOPHT)", Ontario Hydro Report, CNS-37-2, September, 1977.

[5] WAHBA,N.N. and LOCKE,K.E., "Fuel Bundle Impact Velocities due to Reverse Flow", 17th Annual Conference, Canadian Nuclear Society, Fredericton, New Brunswick, Canada, June 9-12, 1996.

[6] WAHBA,N.N., "Factors Affecting Fuel Bundle Movement due to Reverse Flow", Fifth International Conference on Simulation Methods in Nuclear Engineering, Montreal, Canada, September 8-11, 1996.

Table 1
Reference Input Values

Channel Power (kW)	6000
Inlet Header Pressure (MPa)	10.4
Outlet Header Pressure (MPa)	9.2
Inlet Header Enthalpy (kJ/kg)	1074
Outlet Header Enthalpy (kJ/kg)	1298
Channel Elevation (m)	10
Number of Bundles in Channel	13
Bundle Mass (kg)	23.7
Bundle Length (m)	0.495
Bundle Loss Coefficient	0.816
Gap between End Bundle and Shield Plug (m)	0.5
Inlet Feeder Diameter (m)	0.063
Inlet Feeder Length (m)	10
Inlet Feeder Loss Coefficient	1.0
Outlet Feeder Diameter (m)	0.063
Outlet Feeder Length (m)	10
Outlet Feeder Loss Coefficient	1.0
Distance between Break and Inlet End-fitting (m)	0.5
Break Developing Time (ms)	30

FIGURE 1: BUNDLE VELOCITY VS TIME
EFFECT OF GAP BETWEEN END BUNDLE AND SHIELD PLUG

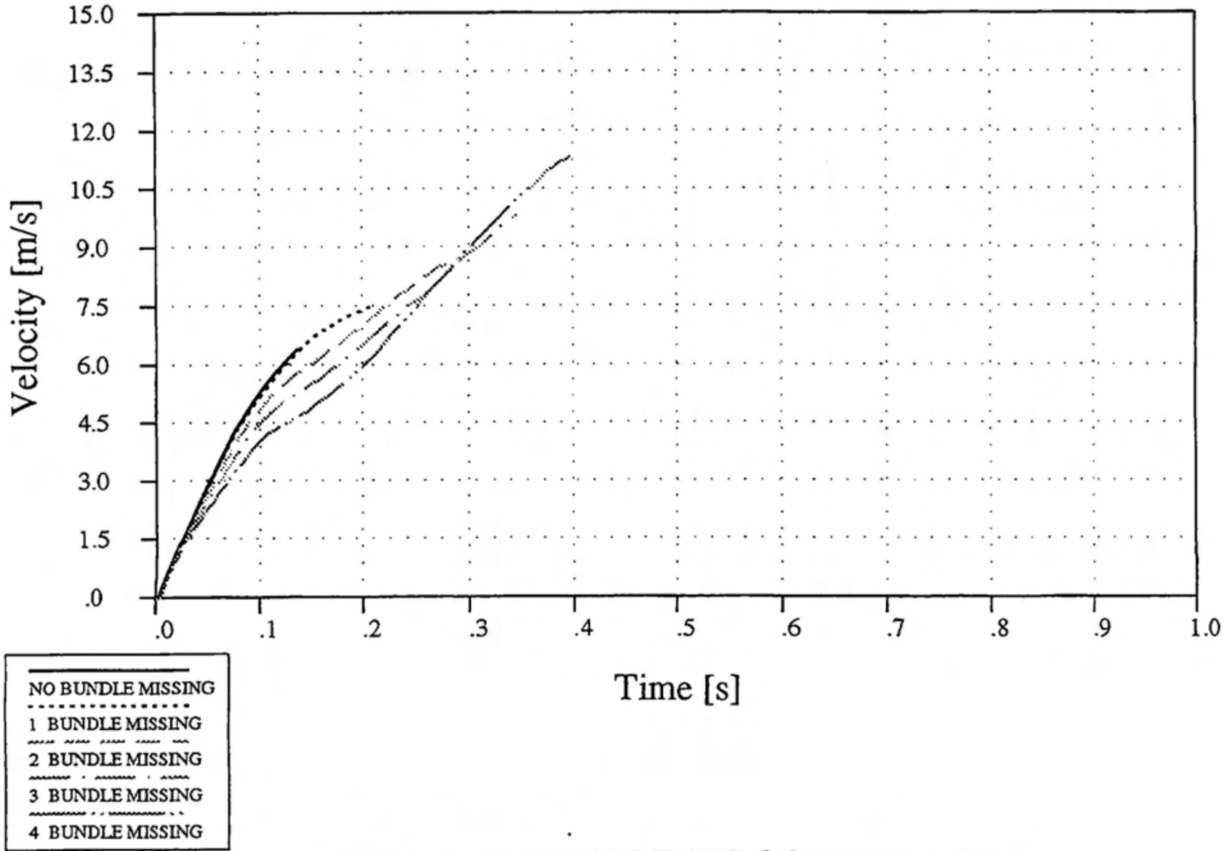

FIGURE 2: BUNDLE VELOCITY VS TIME
EFFECT OF GAP BETWEEN END BUNDLE AND SHIELD PLUG

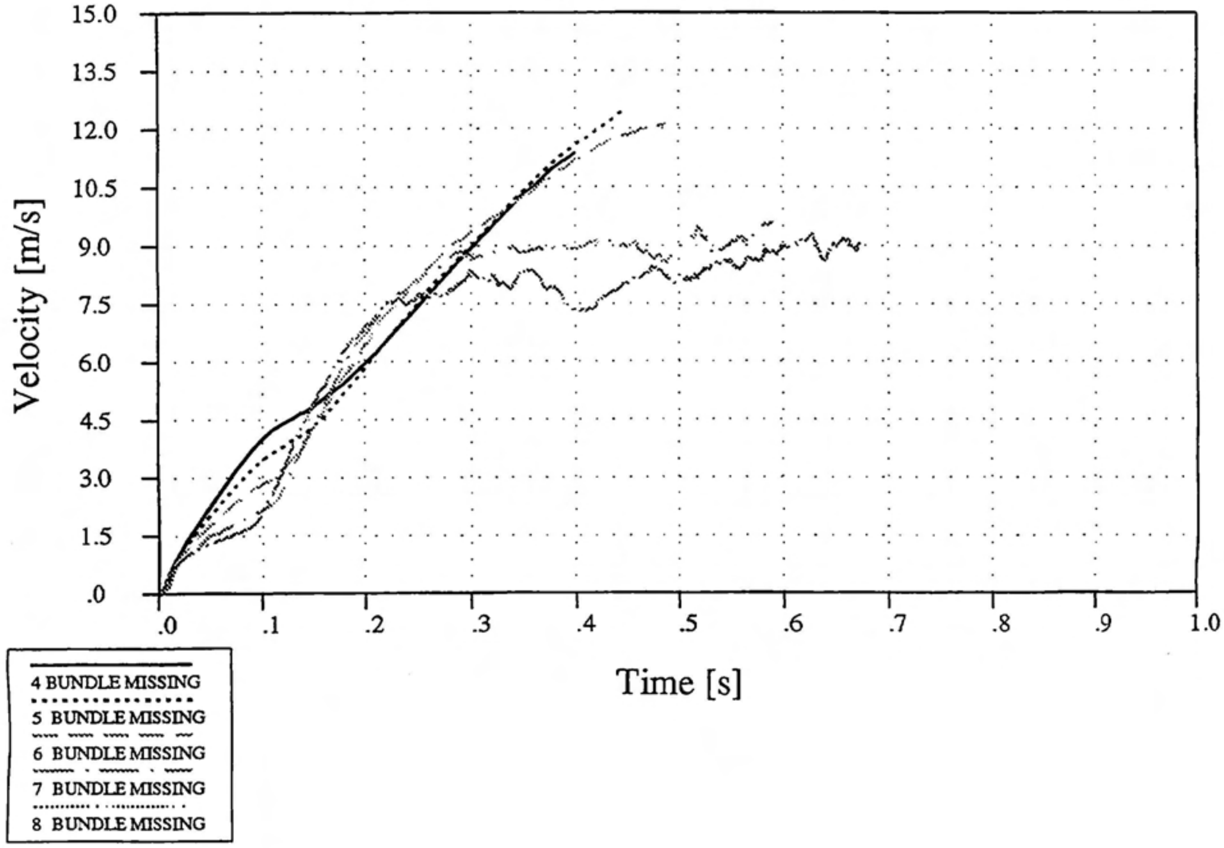

FIGURE 3: BUNDLE VELOCITY VS TIME (NO BUNDLE MISSING)
CHANNEL POWER EFFECT

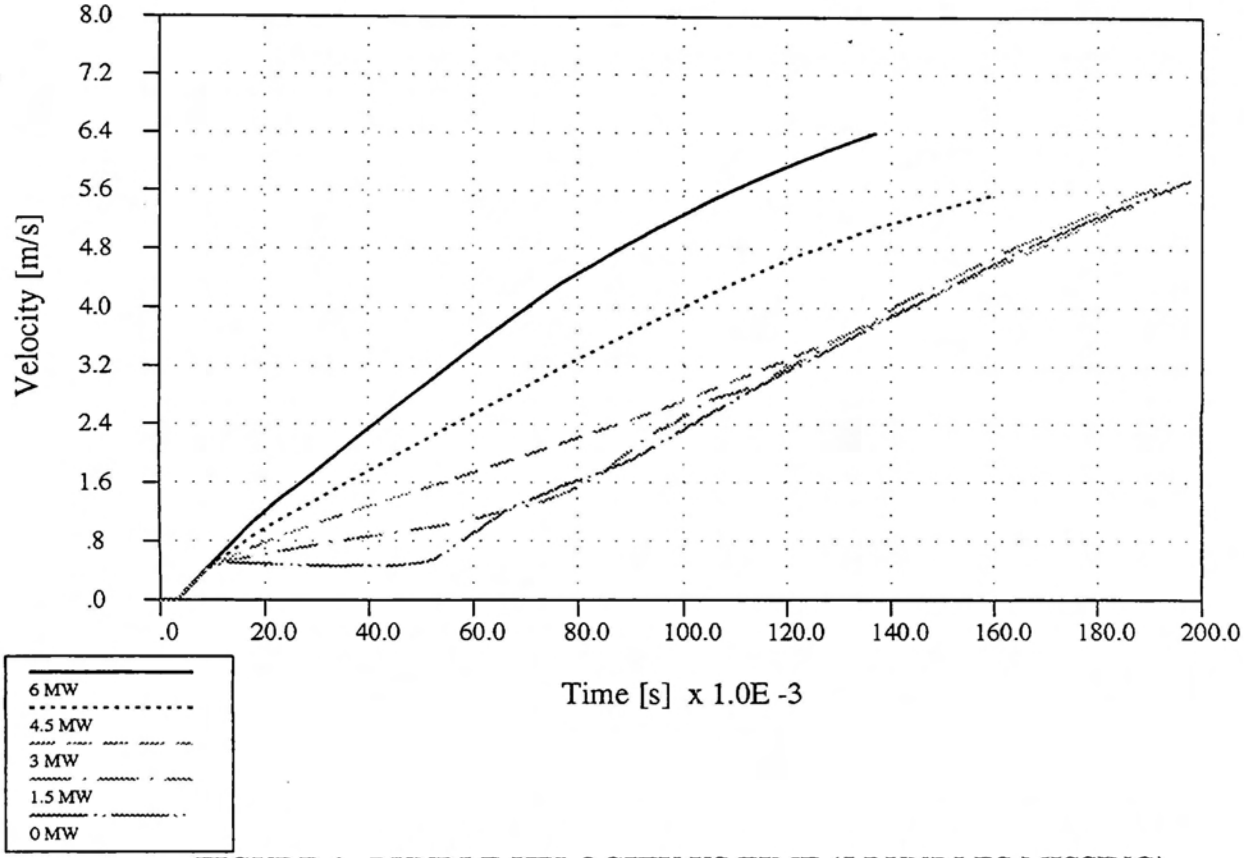

FIGURE 4: BUNDLE VELOCITY VS TIME (5 BUNDLES MISSING)
CHANNEL POWER EFFECT

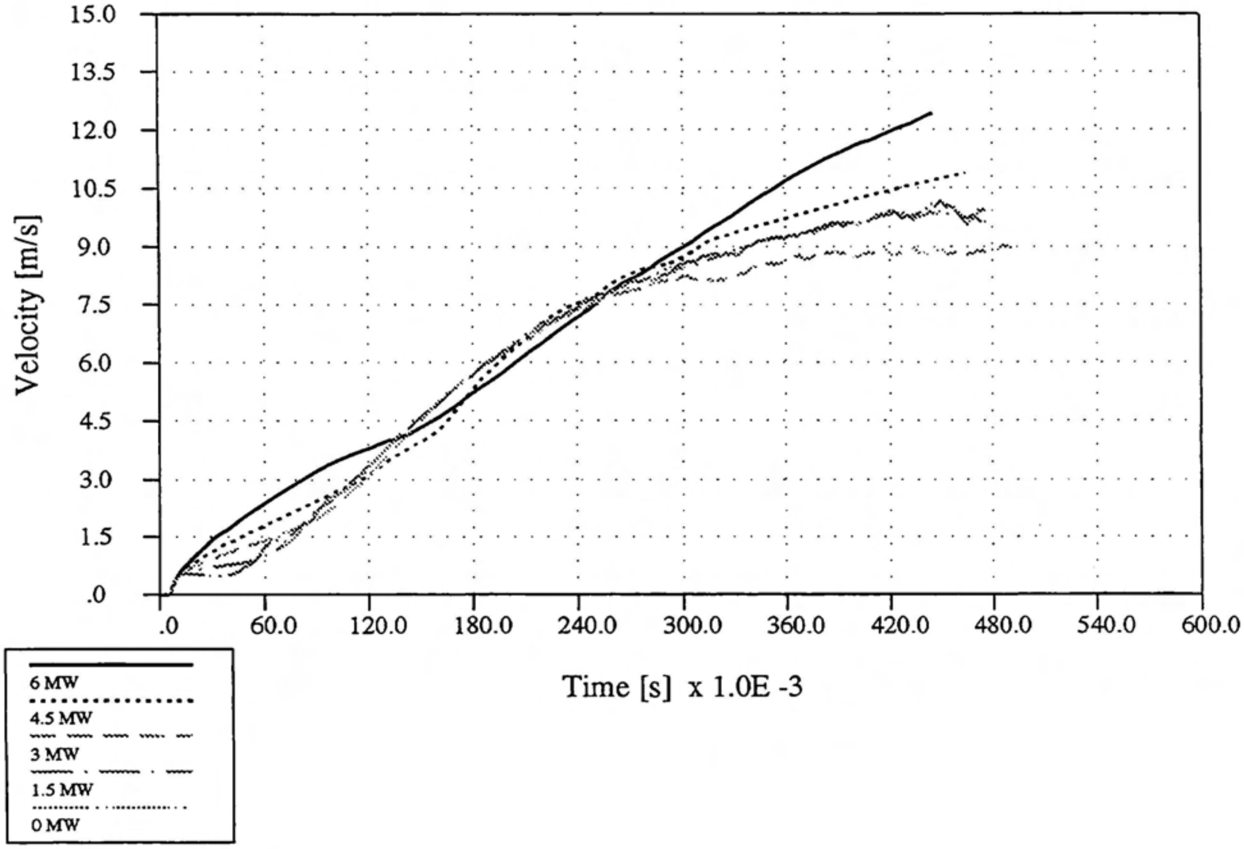

Fri Apr 25 17:08:17 1997
nwahba/rfi-parm/chp/pb-x0

FIGURE 5: BUNDLE VELOCITY VS TIME (NO BUNDLE MISSING)
INLET HEADER ENTHALPY EFFECT-CHANNEL POWER = 0 MW

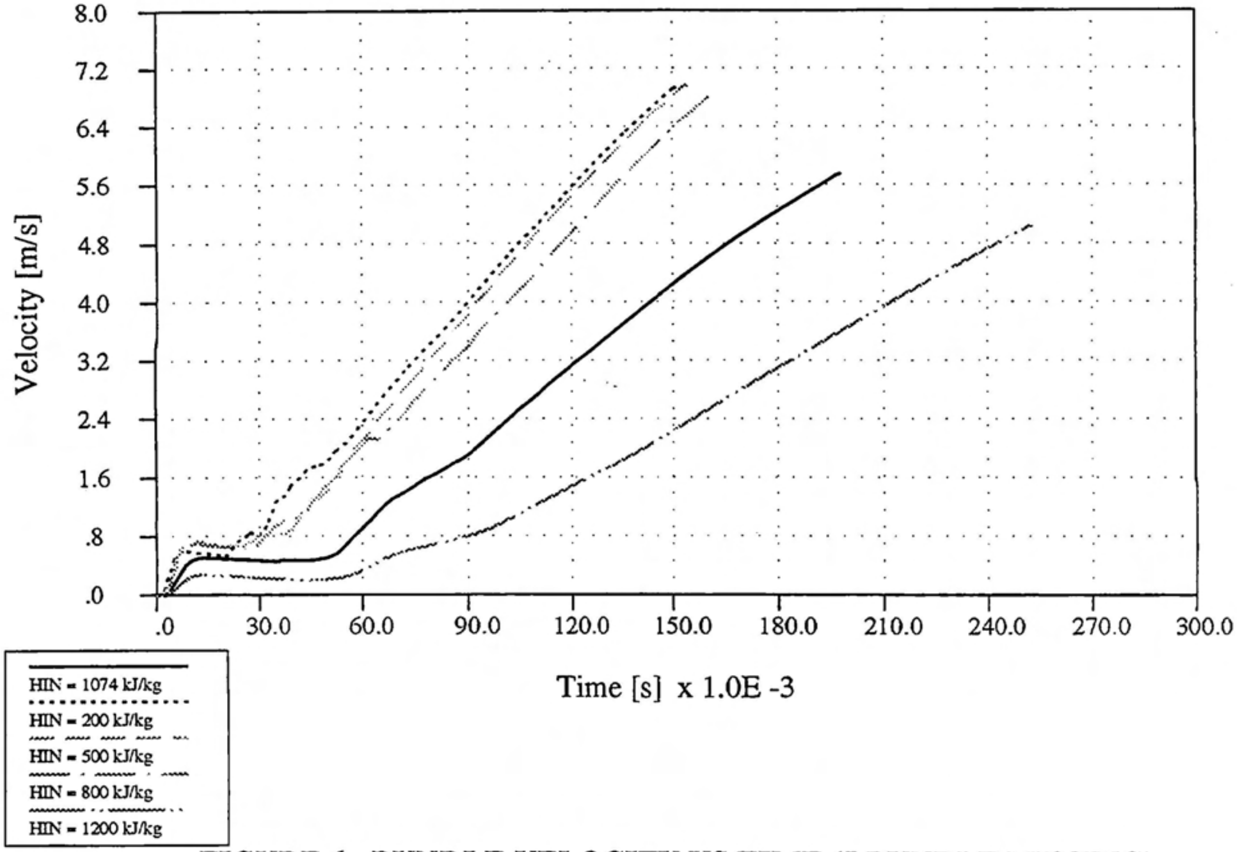

FIGURE 6: BUNDLE VELOCITY VS TIME (5 BUNDLE MISSING)
INLET HEADER ENTHALPY EFFECT-CHANNEL POWER = 0 MW

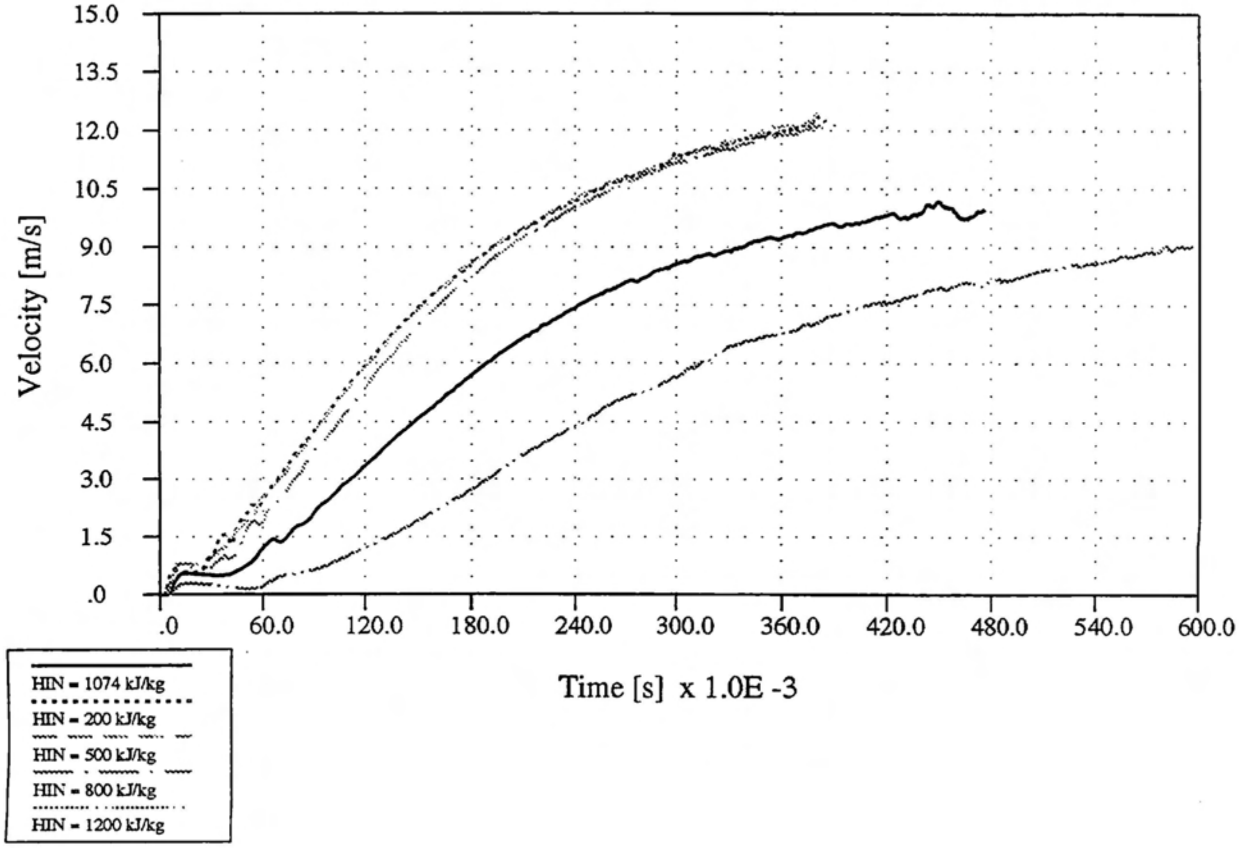

Fri Apr 25 17:24:01 1997
nwahba/rfl-parm/chbi-p0/pb-x0

FIGURE 7: BUNDLE VELOCITY VS TIME (NO BUNDLE MISSING)
INLET HEADER ENTHALPY EFFECT-CHANNEL POWER = 6 MW

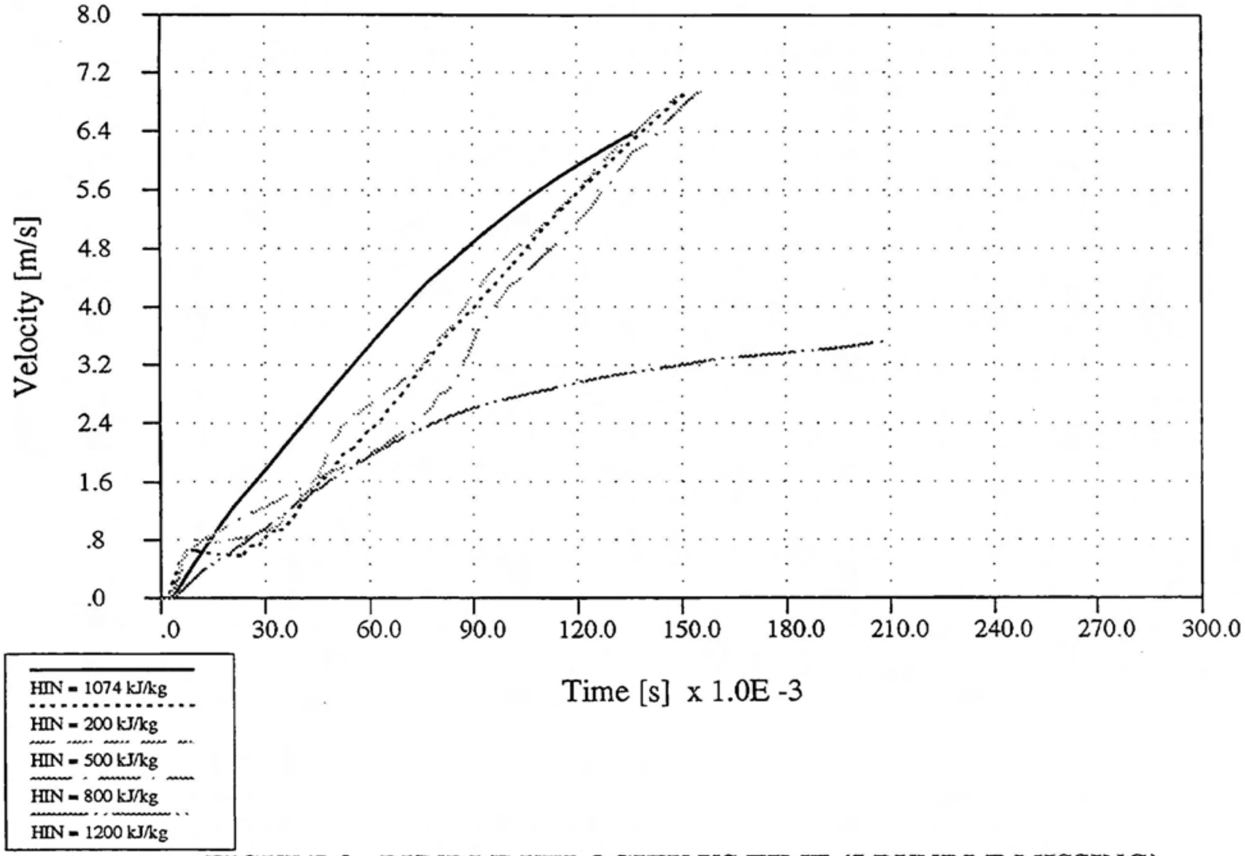

FIGURE 8: BUNDLE VELOCITY VS TIME (5 BUNDLE MISSING)
INLET HEADER ENTHALPY EFFECT-CHANNEL POWER = 6 MW

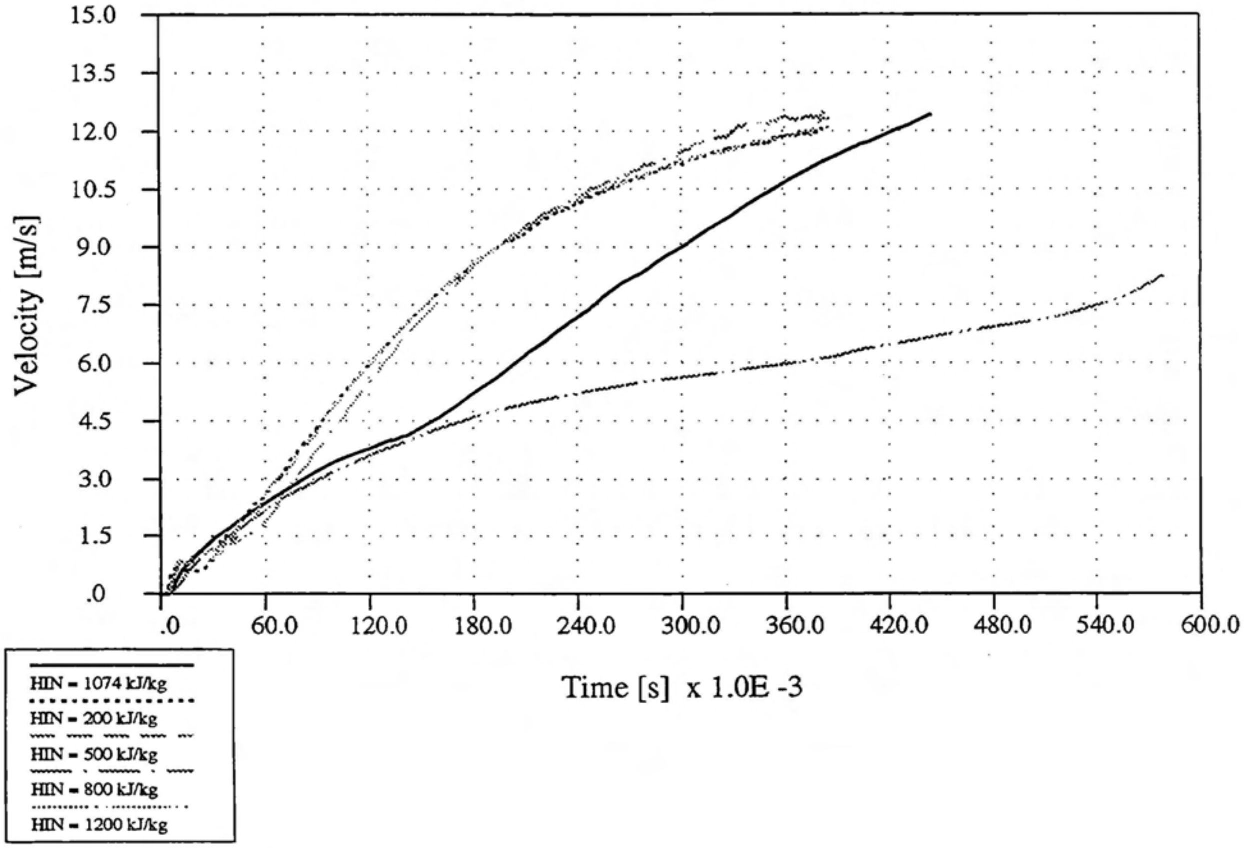

FIGURE 9: BUNDLE VELOCITY VS TIME (NO BUNDLE MISSING)
OUTLET HEADER ENTHALPY EFFECT

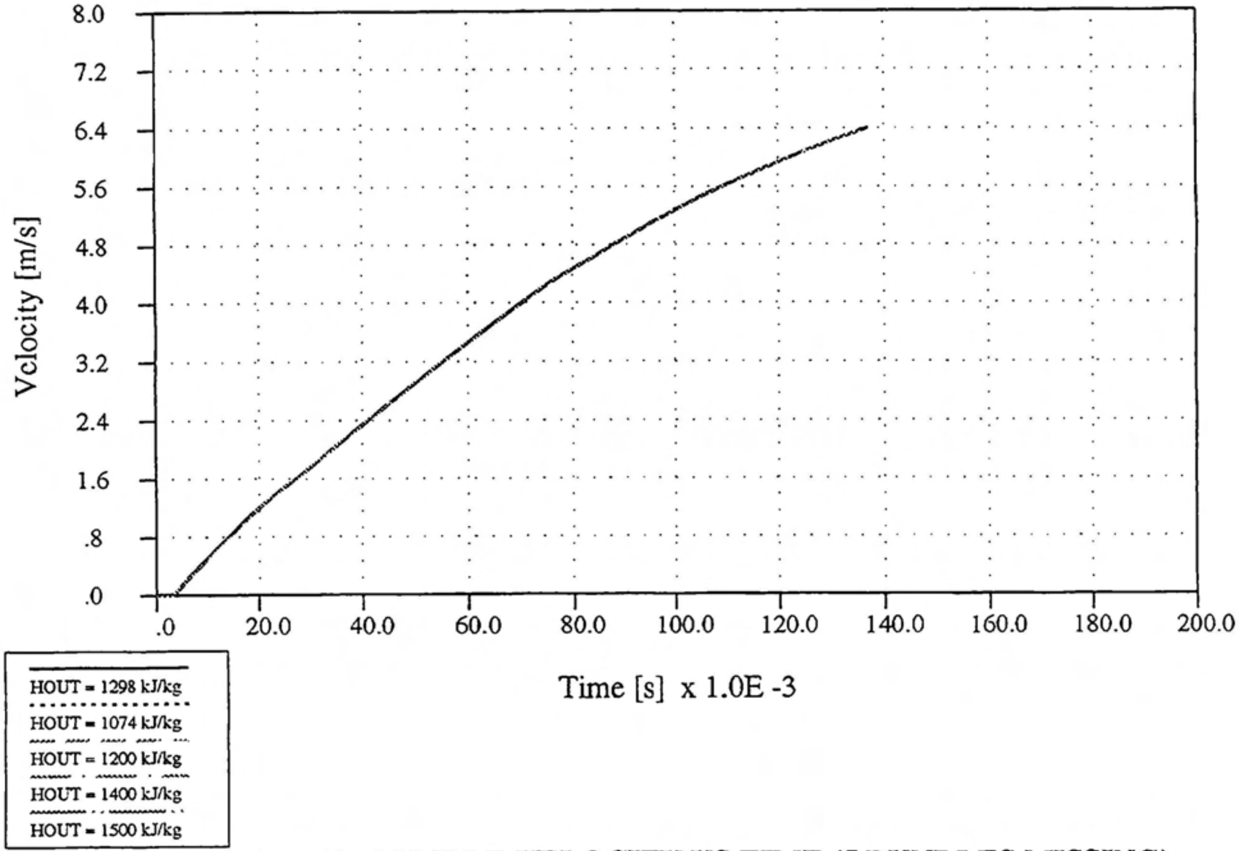

FIGURE 10: BUNDLE VELOCITY VS TIME (5 BUNDLES MISSING)
OUTLET HEADER ENTHALPY EFFECT

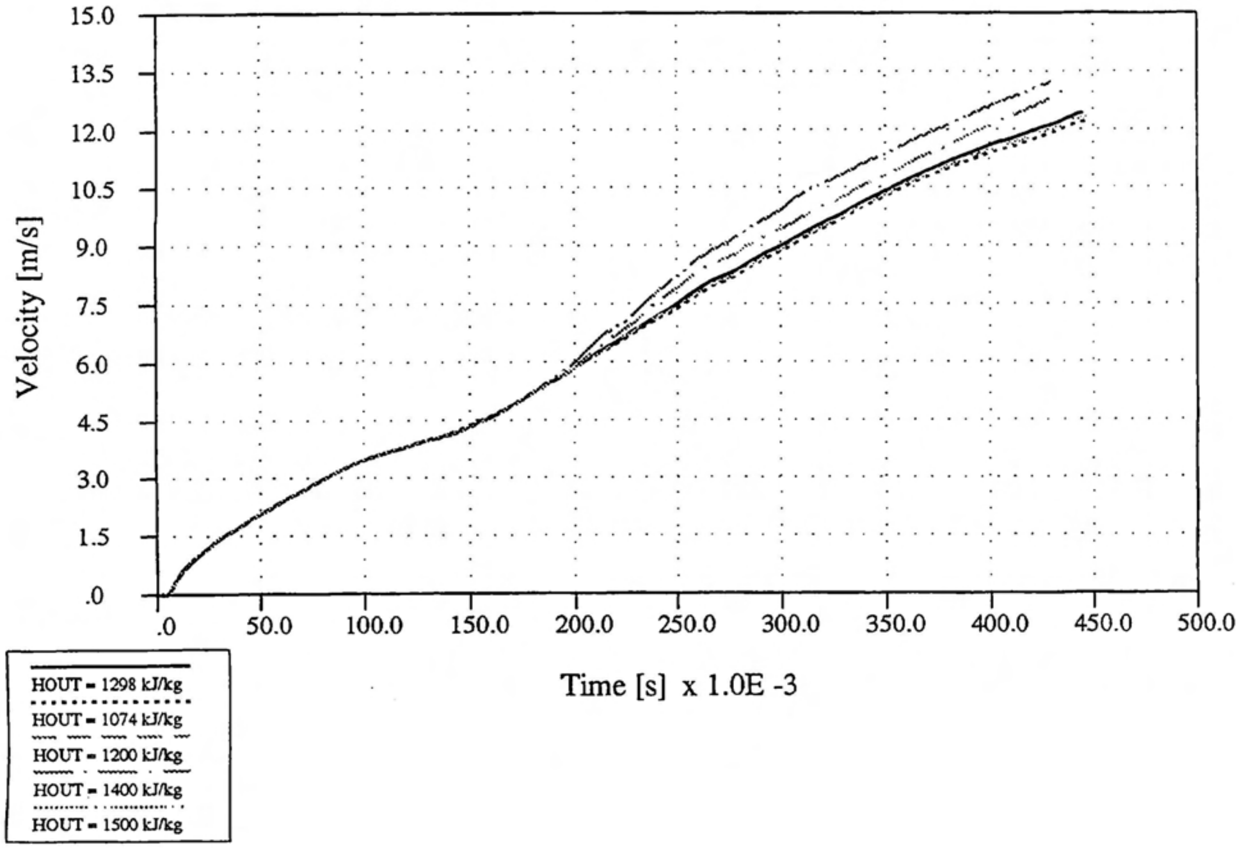

Fri Apr 25 18:11:00 1997
nwabba/rfi-parm/chbo/pb-x0

FIGURE 11: BUNDLE VELOCITY VS TIME (NO BUNDLE MISSING)
CHANNEL PRESSURE EFFECT, DP = 1.2 MPa

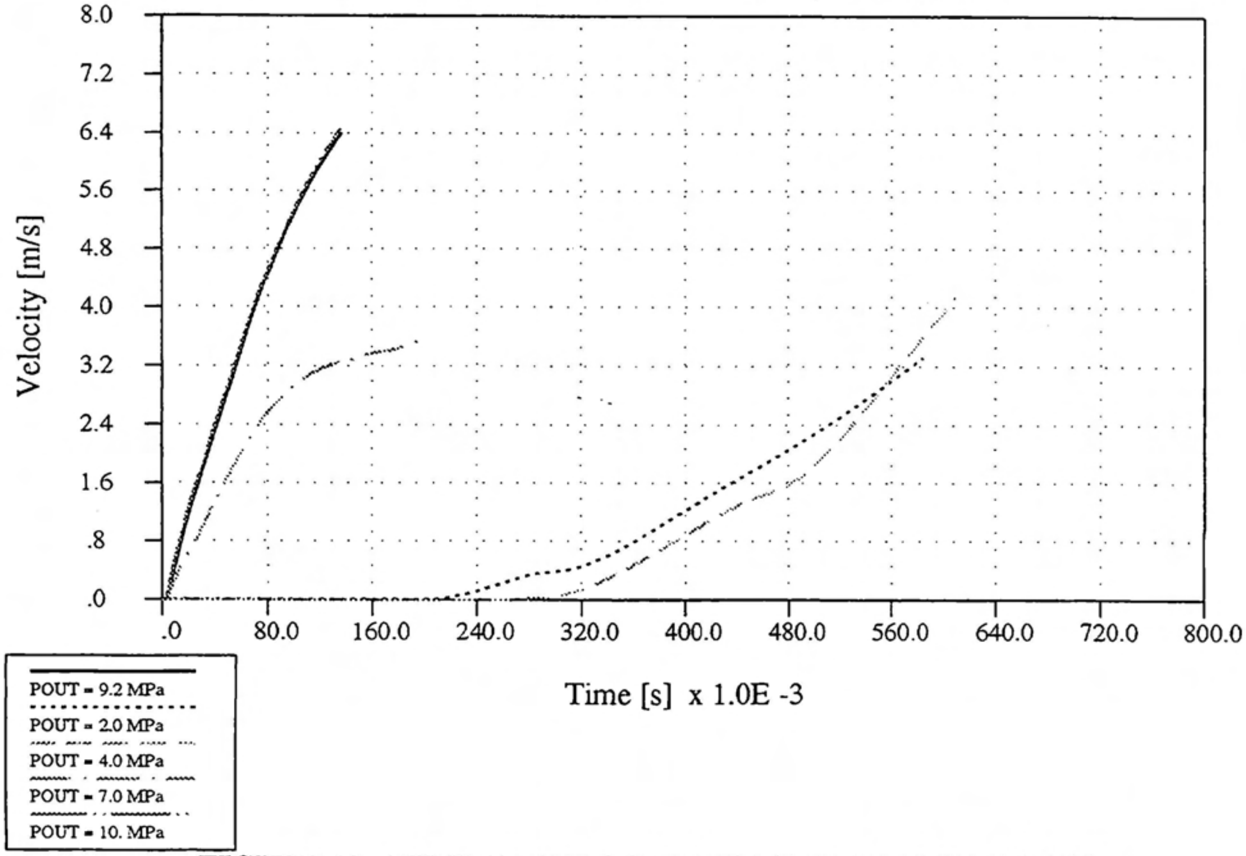

FIGURE 12: BUNDLE VELOCITY VS TIME (5 BUNDLE MISSING)
CHANNEL PRESSURE EFFECT, DP = 1.2 MPa

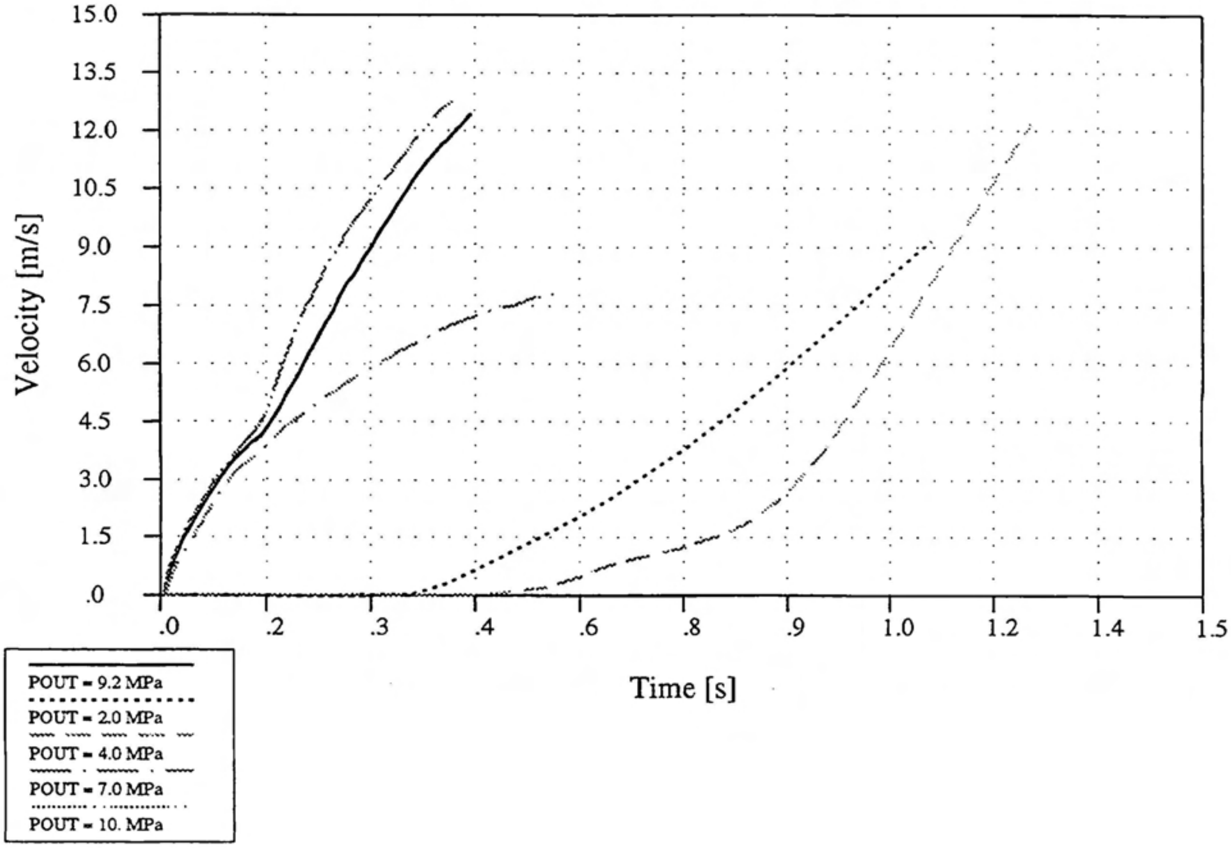

Fri Apr 25 18:21:34 1997
nwahba/rfi-parm/chpres/pb-x0

FIGURE 13: BUNDLE VELOCITY VS TIME (NO BUNDLE MISSING)
HEADER TO HERADER PRESSSURE DROP EFFECT (POUT = 9.2 MPa)

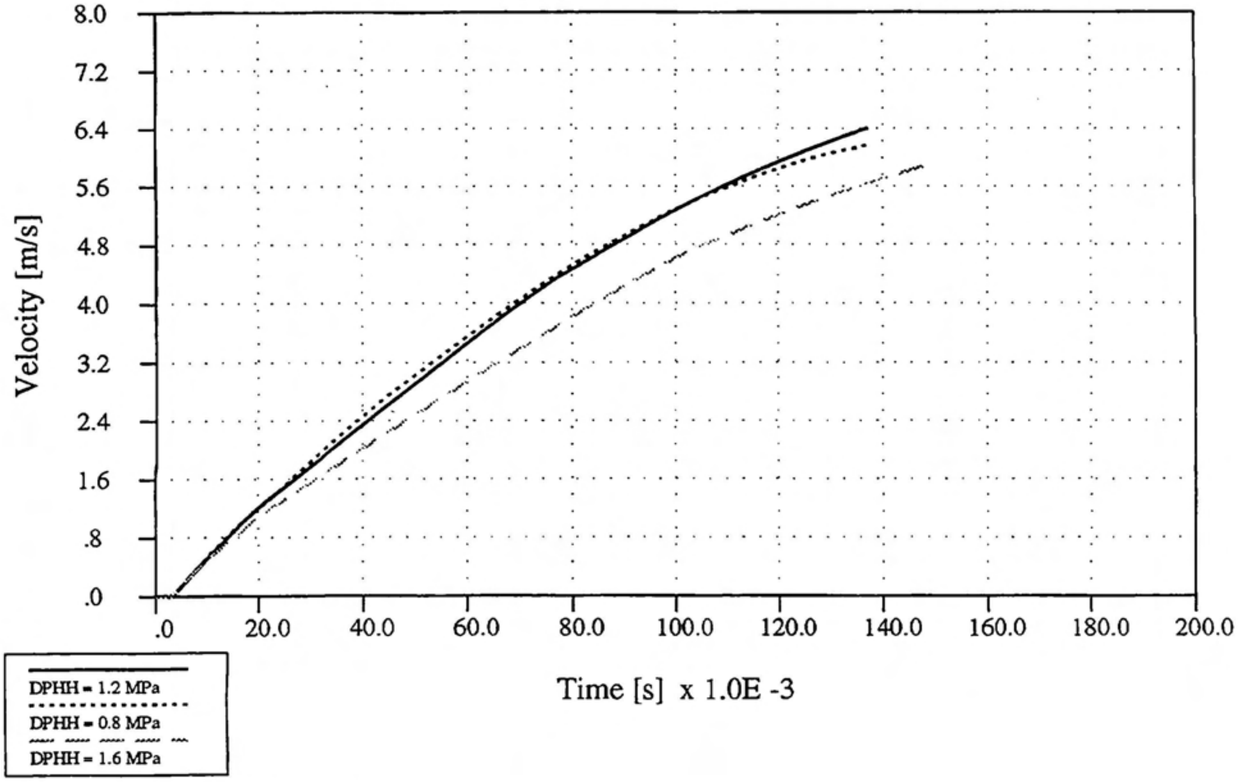

FIGURE 14: BUNDLE VELOCITY VS TIME (5 BUNDLE MISSING)
HEADER TO HERADER PRESSSURE DROP EFFECT (POUT = 9.2 MPa)

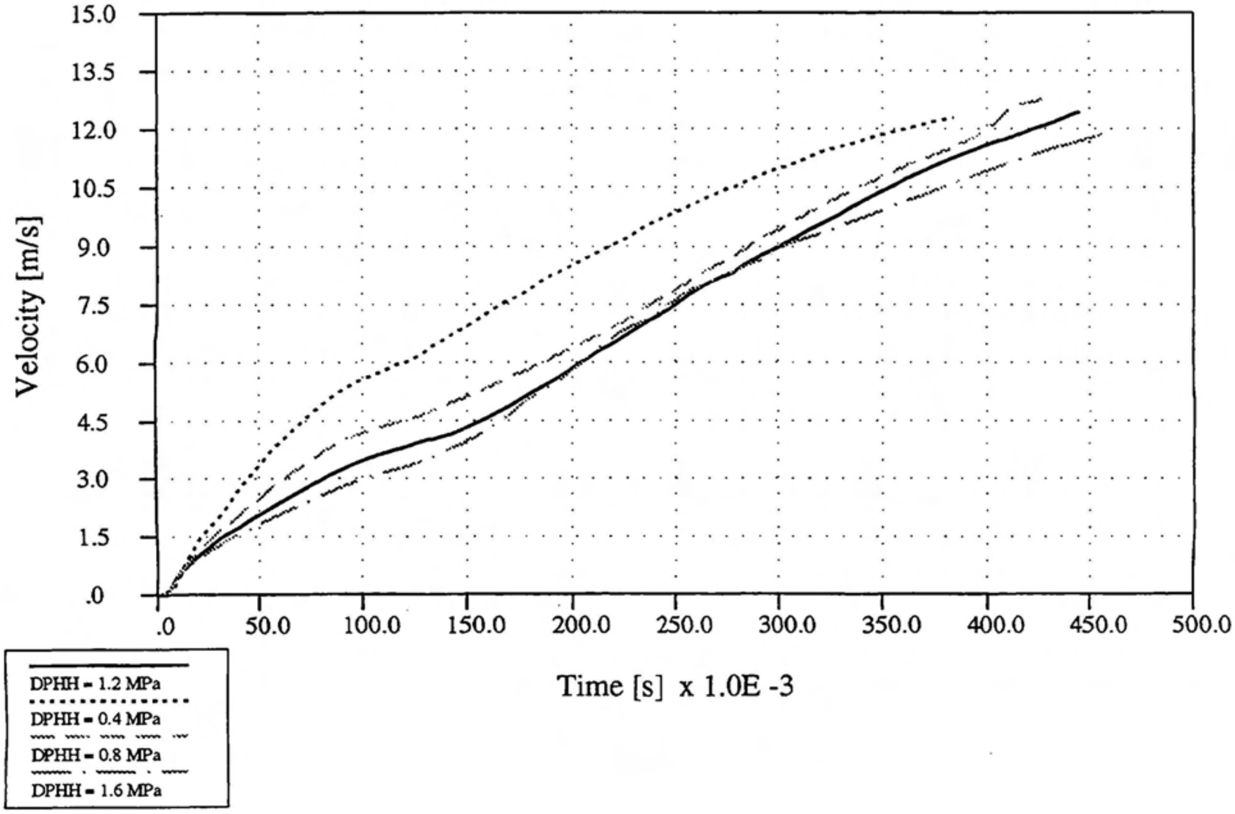

**FIGURE 15: BUNDLE VELOCITY VS TIME (NO BUNDLE MISSING)
HEADER TO HERADER PRESSSURE DROP EFFECT (PIN = 10.4 MPa)**

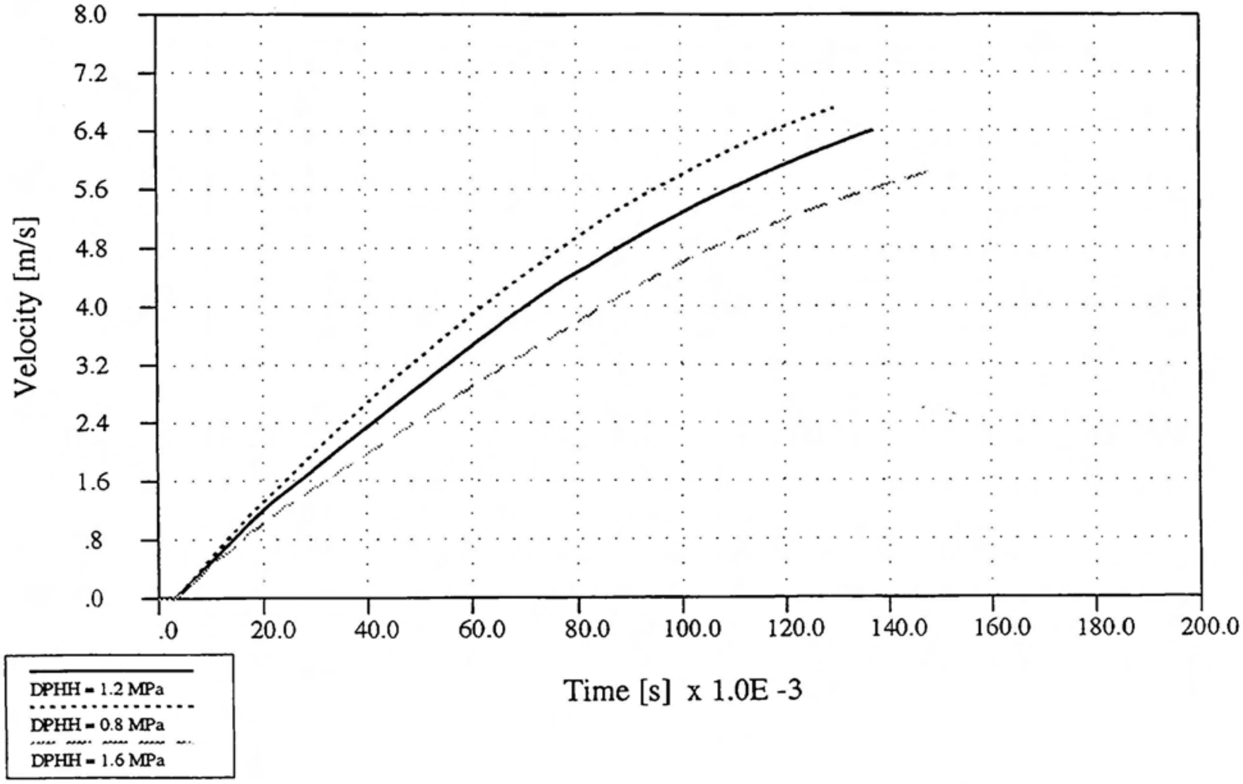

**FIGURE 16: BUNDLE VELOCITY VS TIME (5 BUNDLE MISSING)
HEADER TO HERADER PRESSSURE DROP EFFECT (PIN = 10.4 MPa)**